Macromolecules
ARTICLE

*Macromolecules* **2010**, *43*, 5845–5850 **5845**
DOI: 10.1021/ma100383r

# Influence of Pressure on Chain and Segmental Dynamics in Polyisoprene

**Sebastian Pawlus,*,[†] Alexei P. Sokolov,[‡] Marian Paluch,[†] and Michal Mierzwa[†]**

[†]*Institute of Physics, University of Silesia, Uniwersytecka 4, 40-007 Katowice, Poland, and*
[‡]*Chemical Sciences Division, ORNL, and Department of Chemistry, University of Tennessee, Knoxville, Tennessee 37996-1600*

*Received February 17, 2010; Revised Manuscript Received April 27, 2010*

ABSTRACT: We present detailed studies of variation in segmental and chain dynamics of polyisoprene under pressure. Samples with two molecular weights (MW), 2.4 and 25 kg/mol (below and above entanglement), were investigated. Dielectric spectroscopy measurements at isobaric and isothermal conditions exhibit clear differences in temperature and pressure dependencies of chain and segmental relaxation times. Moreover, application of pressure increases time separation between the segmental and normal (chain) modes at the isochronic conditions. This increase can be explained by an effective increase in number of Rouse segments under compression at the same segmental relaxation time. Our analysis also reveals that the thermodynamic scaling of the relaxation times (log $\tau$ vs $TV^{\gamma}$, $V$ is volume) does not work well simultaneously for both processes.

## Introduction

Because of chain connectivity polymers exhibit a specific only for them relaxation process—chain relaxation (or normal modes). Chain modes have relaxation times significantly longer than that of segmental (structural) relaxation and define the unique viscoelastic properties of polymers.[1] Chain modes are usually well described by the Rouse model for nonentangled polymers and by reptation model for entangled chains.[2] Both models are based on assumption of some chain friction coefficient that is traditionally assumed to be the same as the monomeric friction controlling segmental relaxation.[2] In that case, temperature variations of the characteristic chain and segmental relaxation times are expected to be similar.[2] This assumption is the basis for the time–temperature superposition (TTS) principle. However, the break down of TTS at temperatures approaching the glass transition, $T_g$, is well-known: chain relaxation exhibits weaker temperature variations than the segmental one.[3]

Polymer dynamics is usually studied as a function of temperature at ambient pressure. In that case both, change of density and thermal energy, contribute to the slowing down of relaxation processes.[2] Relative contribution of these two thermodynamic variables can be estimated using measurements and simulations of dynamics under pressure.[4−12] Many high pressure investigations have been applied to studies of segmental dynamics.[5−10,13−19] In contrast to our traditional vision of applicability of free volume ideas to polymers, they demonstrated that volume play a minor role in slowing down of segmental relaxation in most of the polymers.[5,16,17] Its role, however, increases with decrease in molecular weight. This result indicates importance of intramolecular energy barriers in slowing down of the segmental relaxation in polymers.

Only a few papers analyzed the influence of pressure on chain relaxation.[1,4,12,20−25] They revealed that segmental and chain relaxations show different dependence on pressure, i.e. they exhibit breakdown of time-pressure superposition (TPS),[4,21−23] similar to the breakdown of the TTS. This result again indicates a difference in segmental and chain friction mechanisms. However, analysis by Roland and co-workers revealed some similarities in scaling of chain and segmental relaxation times.[22,24] So, the influence of density on chain relaxation remains poorly studied.

This paper focuses on detailed studies of the influence of pressure (density) on steepness of thermal variations of chain and segmental dynamics in polyisoprene (PIP). We use dielectric spectroscopy to probe both chain and segmental dynamics in the same experiment (it covers extremely broad frequency range) without assumptions of any TTS or TPS. We demonstrate that the steepness of temperature variations (fragility) of segmental dynamics does not exhibit any significant variations with pressure. Most important, our analysis shows that the separation of characteristic relaxation times of chain and segmental modes increases with pressure at isochronic conditions. This effect is similar to an increase in molecular weight of the polymer. Finally we found that the so-called thermodynamic scaling does not work well simultaneously for both modes. All these results emphasize a difference in chain and segmental friction mechanisms.

## Experimental Section

For our studies, we chose polyisoprene, because this polymer has dipole moment accumulating along the chain and its normal modes can be studied using dielectric spectroscopy.[26,27] 1,4-Polyisoprenes with molecular weight (MW) $M_n = 2410$ ($M_W = 2450$, PDI = 1.02; from Scientific Polymer) and $M_n = 25\,000$ ($M_W = 26\,000$, PDI = 1.04; from Polymer Service) have been studied.

Dielectric spectra in the frequency range from 10 mHz up to 3 MHz were measured using Novocontrol Alpha impedance analyzer. For measurements at ambient pressure, the samples were placed in a parallel plate stainless steel capacitor with diameter 20 mm. Teflon spacer maintained distance between electrodes with thickness 0.1 mm. The sample was placed in a cryostat. Novocontrol Quatro Cryosystem controlled temperature with accuracy better than 0.1 K. Pressure measurements were performed using the system constructed in cooperation with UNIPRESS and described elsewhere.[28] Samples were placed in a capacitor with diameter and distance between plates the same as in ambient pressure measurements and sealed by the Teflon ring to separate from pressurized medium. Pressure was exerted on the sample by Sitec hydraulic press via silicon oil. Temperature of the sample was controlled with accuracy 0.5 K by means of a liquid flow from thermostatic bath.

---

*Corresponding author.

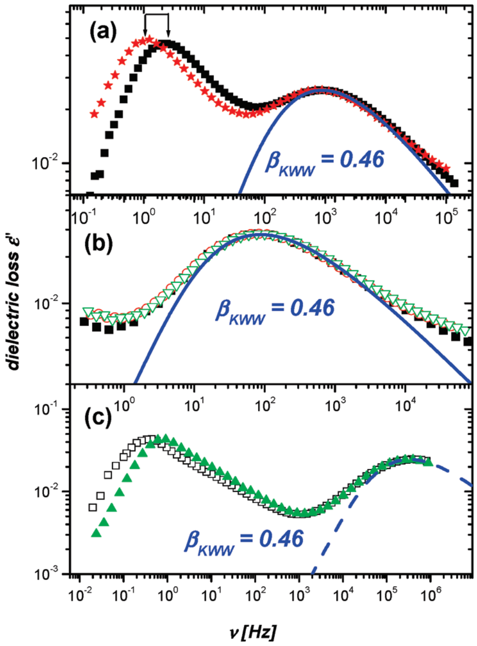

**Figure 1.** Spectral shape comparison of the segmental and chain process in PI with (a) MW = 2.4K (black squares, $P = 0.1$ MPa, $T = 223$ K; red stars, $P = 405$ MPa, $T = 288.3$K) and (b, c) MW = 25K at different thermodynamic conditions but for the same segmental relaxation times (b, black squares, $P = 0.1$ MPa, $T = 222$ K; red circles, $P = 302$ MPa, $T = 275.55$ K; green triangles, $P = 196$ MPa, $T = 259.65$ K; c, green triangles, $P = 0.1$ MPa, $T = 252.15$ K; black squares, $P = 302$ MPa, $T = 309.75$ K).

## Results and Discussion

The dielectric loss spectra of PIP exhibit two pronounced peaks (Figure 1): the low-frequency one is related to the chain relaxation and the higher frequency one originates from the segmental relaxation. The two representative spectra depicted in Figure 1a have been measured in PIP with MW = 2.4K at different $P-T$ conditions and chosen to have the same segmental relaxation time. We fit segmental relaxation spectra by the Fourier transformation of Kohlrausch−Williams−Watts (KWW) functions, $\phi(t) = \exp[-(t/\tau)^{\beta}{}_{KWW}]$. For both samples the stretching exponent is $\beta_{\mathrm{KWW}} = 0.46 \pm 0.02$, and it remains essentially temperature and pressure independent (Figure 1).

Characteristic relaxation times were determined from the frequency of the maximum of the loss peaks, $\tau = (2\pi f_{max})^{-1}$. The obtained relaxation times for both chain ($\tau_{\mathrm{C}}$) and segmental ($\tau_{\mathrm{S}}$) modes at different isothermal conditions are shown in Figure 2a for MW = 2.4K and in Figure 2b for MW = 25K. Contrary to the earlier results by Floudas et al.,[4,21] pressure behavior of both relaxations has clearly nonlinear character and can be described by pressure counterpart of the temperature Vogel−Fulcher−Tamman (VFT) equation.[29,30] The difference between our and the Floudas et al results comes from the different temperature and a broader pressure ranges used in our studies. As a result, we were able to monitor pressure behavior of both relaxation modes in a much wider time range.

Pressure dependence is often characterized by the activation volume $\Delta V$ (similar to the activation energy for temperature variations) defined as

$$\Delta V = 2.303RT\left(\frac{\partial \log \tau}{\partial P}\right)_T$$

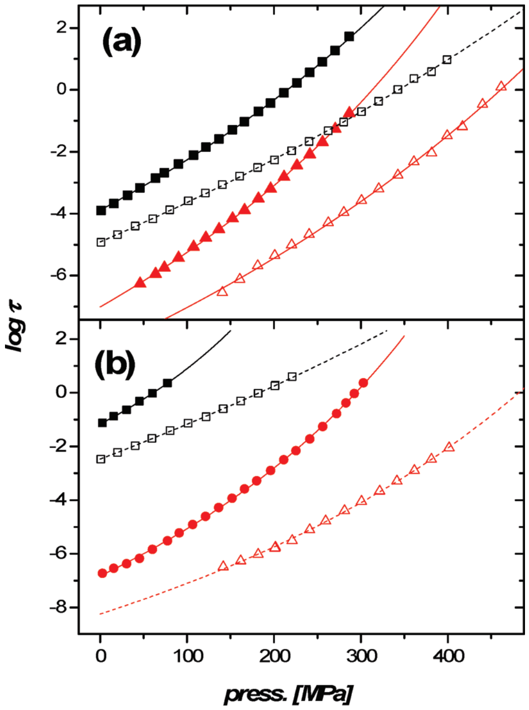

**Figure 2.** Pressure dependences of the segmental and the chain relaxation times for (a) MW = 2.4K (filled triangles, $\tau_{\mathrm{s}}$ at 254.5 K; filled squares, $\tau_{\mathrm{C}}$ at 254.5 K; empty squares, $\tau_{\mathrm{C}}$ at 272.5 K; empty triangles, $\tau_{\mathrm{s}}$ at 272.5 K) and (b) MW = 25K (empty squares, $\tau_{\mathrm{s}}$ at 259.5 K; filled circles, $\tau_{\mathrm{C}}$ at 259.5 K; empty squares, $\tau_{\mathrm{C}}$ at 283 K; empty triangles, $\tau_{\mathrm{s}}$ at 283 K). Solid lines represent fits with the pressure version of the VFT relation.

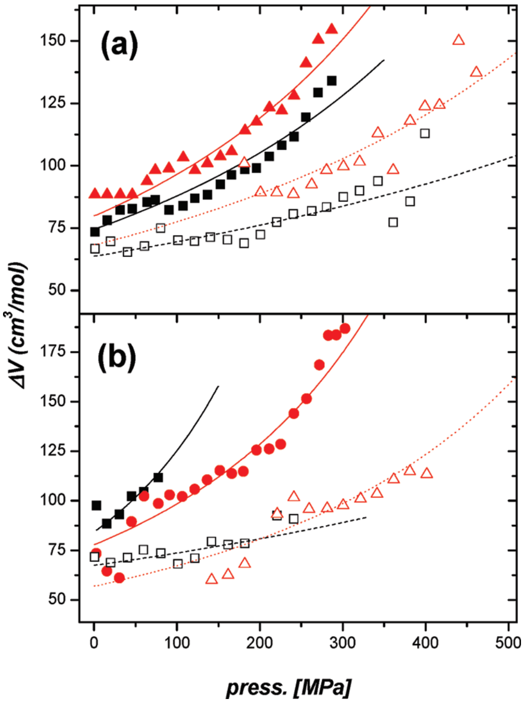

**Figure 3.** Pressure behavior of the activation volume, $\Delta V$, for samples with (a) MW = 2.5k (filled squares, $\tau_{\mathrm{C}}$ at 254.5 K; filled triangles, $\tau_{\mathrm{s}}$ at 254.5 K; empty squares, $\tau_{\mathrm{n}}$ at 272.5 K; empty triangles, $\tau_{\mathrm{s}}$ at 272.5 K) and (b) MW = 25K (filled squares, $\tau_{\mathrm{C}}$ at 259.5 K; filled circles, $\tau_{\mathrm{s}}$ at 259.5 K; empty squares, $\tau_{\mathrm{C}}$ at 283 K; empty triangles, $\tau_{\mathrm{s}}$ at 283 K).

We estimated values of $\Delta V$ based on the isothermal data (Figure 2). For low-MW sample, values of $\Delta V$ (Figure 3a) are higher for segmental than for chain relaxation and increase during isothermal densification. This observation agrees with previous findings in ref.[4] However, the observed increase of $\Delta V$ with pressure provides additional proof for a nonactivated character of pressure behavior of relaxation dynamics for both processes. This observation becomes obvious due to wider time range used in our studies in comparison to the earlier results presented in.[4,21] For the sample with higher MW (Figure 3b) the picture is unclear: although, similar to the low-MW sample, the activation volume increases with increasing pressure and decreasing temperature, it seems that $\Delta V$ of the normal mode is about the same or even higher than $\Delta V$ of segmental one. However, the limited range where the data for both relaxation times overlaps prevents us from any clear conclusion in that case. It is worth noting that for isotherms at $T$ = 272.5 K and 283 K for MW = 2.4K and 25K, respectively, activation volume at ambient pressure is slightly lower than monomer volume (ca. 75 cm$^3$/mol). As was shown in,[21] $\Delta V$ increases with decreasing temperature. As a result, the values of $\Delta V$ at ambient pressure are higher than the monomer volume in the case of the low temperature isotherms at $T$ = 254.5 K and 259.5 K for MW = 2.4K and 25K, respectively.

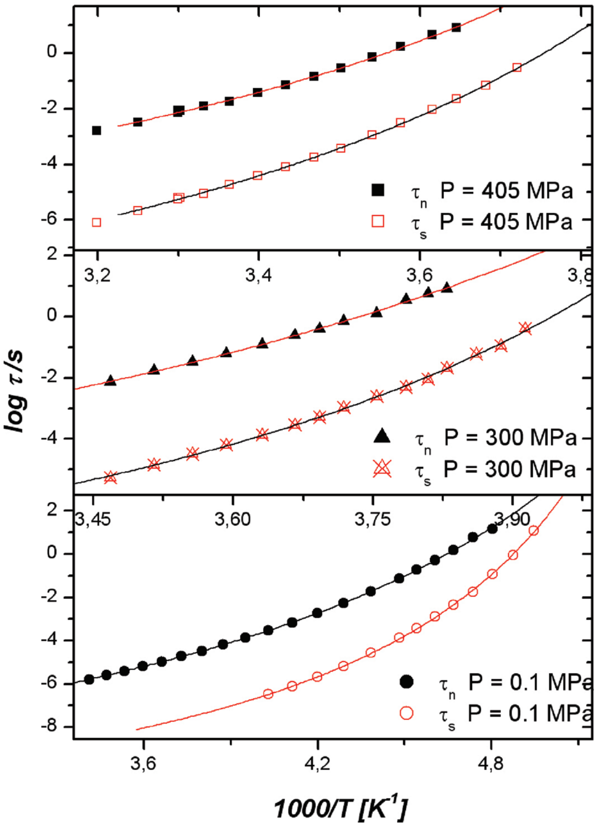

**Figure 4.** Arrhenius plot of the segmental and chain relaxation times measured isobaricaly in PI with MW = 25K at 400 MPa (upper panel), 300 MPa (middle panel) and 0.1 MPa (lower panel). Solid lines represent fits by the VFT relations.

Let us now focus on analysis of temperature variations of relaxation times at different pressures. In Figure 4 the temperature dependences of relaxation times for both processes are presented for the sample with MW = 25K. It is clear that all isobaric dependencies of relaxation times have non-Arrhenius character and consequently they were fitted to the VFT equation. The same picture is observed for low-MW sample (not presented here). The VFT parameters for all pressure conditions and molecular weights are collected in the Table 1. Steepness of the temperature variations of segmental relaxation is usually characterized by fragility parameter $m$ defined as:

$$m = \frac{d \log \tau_s}{d\left(\frac{T_g}{T}\right)_{Tg}} \tag{1}$$

It characterizes the deviation of the temperature dependence from an Arrhenius behavior.[31] Higher $m$ indicates stronger non-Arrhenius behavior. Figure 5 presents the relaxation times vs $T_g$/T for both samples. To avoid extrapolation of the data much above accessible temperature range, the $T_g$ has been defined as the temperature at which segmental relaxation time $\tau_S$ = 10 s. In the case of a sample with MW = 2.4K (< $M_e$), the steepness index remains pressure independent and equal to 77 ± 5 (Figure 5a). For the sample with MW > $M_e$ the pattern of behavior is similar: the fragility remains essentially the same for all isobaric conditions and equal ca. $m$ = 70 ± 5 (Figure 5b).

Recent studies suggest that the temperature variation of the chain relaxation presented vs $T_g/T$ is almost universal for many polymers.[32] Although this universality has been questioned in ref 33, it is obvious that the value of "effective" fragility of chain relaxation is less sensitive to polymeric chemical structure than the fragility of segmental relaxation.[32,34] Presented here results suggest that the $T_g$-scaled temperature behavior of the chain relaxation times is not only weakly affected by polymeric structure and molecular weight, but also by the densification of the sample.

The glass transition temperature exhibits a nonlinear dependence on pressure for both low- and high- MW samples (Figure 6). It can be described by the empirical equation[20] which has been

**Table 1. Main fit parameters for both isobaric and isothermal data of PIP samples with two molecular weights**

| MW | $T$, $P$ | range | $T_g$ [10 s] K | $m$ | $\log \tau_\infty$ | $D_T$ | $T_0$ [K] | $\log \tau_0$ | $D_p$ | $P_0$[MPa] |
|---|---|---|---|---|---|---|---|---|---|---|
| 2.4K | 0.1 MPa$_{seg.}$ | 201.15−273.15K | $202.2_{\pm1}$ | $76_{\pm2}$ | $-12.3_{\pm0.15}$ | $2.8_{\pm0.1}$ | $166.7_{\pm1.1}$ | | | |
| | 0.1 MPa$_{chain}$ | 201.15−273.15K | | | $-10.7_{\pm0.1}$ | $5.1_{\pm0.15}$ | $146.8_{\pm1.1}$ | | | |
| | 300 MPa$_{seg.}$ | 255.5−288.3K | $250.2_{\pm2}$ | $77_{\pm3}$ | $-12.1_{\pm0.6}$ | $2.7_{\pm0.4}$ | $207.8_{\pm3.9}$ | | | |
| | 300 MPa$_{chain}$ | 255.5−288.3 K | | | $-9.9_{\pm1.1}$ | $4.0_{\pm1.1}$ | $191.6_{\pm9.1}$ | | | |
| | 405 MPa$_{seg.}$ | 303−344 K | $262.5_{\pm2}$ | $73_{\pm3}$ | $-13.7_{\pm0.4}$ | $3.9_{\pm0.4}$ | $207.6_{\pm3.0}$ | | | |
| | 405 MPa$_{chain}$ | 303−344 K | | | $-9.7_{\pm0.2}$ | $3.7_{\pm0.5}$ | $203.5_{\pm2.3}$ | | | |
| | 254.35 K | 1−287 MPa | | | | | | $-7.01_{\pm0.02}$ | $18_{\pm1}$ | $1103_{\pm45}$ |
| | 254.35 K | 1−287 MPa | | | | | | $-3.08_{\pm0.2}$ | $19_{\pm1}$ | $1265_{\pm54}$ |
| | 272.5 K | 1−461 MPa | | | | | | $-8.4_{\pm0.1}$ | $22_{\pm4}$ | $1657_{\pm200}$ |
| | 272.5 K | 1−461 MPa | | | | | | $-4.92_{\pm0.02}$ | $29_{\pm2}$ | $2343_{\pm154}$ |
| 25K | 0.1 MPa$_{seg.}$ | 207.15−333.15K | $206.6_{\pm1}$ | $66_{\pm2}$ | $-17.7_{\pm0.2}$ | $4.2_{\pm0.2}$ | $160.7_{\pm1.1}$ | | | |
| | 0.1 MPa$_{chain}$ | 207.15−333.15K | | | $-7.6_{\pm0.1}$ | $3.9_{\pm0.1}$ | $161.4_{\pm0.8}$ | | | |
| | 302 MPa$_{seg.}$ | 259.5−359.3 K | $257_{\pm2}$ | $71_{\pm3}$ | $-14.2_{\pm0.2}$ | $4.2_{\pm0.2}$ | $201.9_{\pm1.5}$ | | | |
| | 302 MPa$_{chain}$ | 259.5−359.3 K | | | $-6.3_{\pm0.2}$ | $2.3_{\pm0.2}$ | $222.2_{\pm3.0}$ | | | |
| | 350 MPa$_{seg.}$ | 258−369.1 K | $263_{\pm2}$ | $72_{\pm3}$ | $-13.9_{\pm0.3}$ | $3.9_{\pm0.3}$ | $208.5_{\pm2.0}$ | | | |
| | 350 MPa$_{chain}$ | 258−369.1 K | | | $-6.5_{\pm0.1}$ | $2.6_{\pm0.2}$ | $224.5_{\pm2.5}$ | | | |
| | 259.5 K | 2.9−303 MPa | | | | | | $-6.82_{\pm0.02}$ | $14.1_{\pm0.6}$ | $902_{\pm27}$ |
| | 259.5 K | 2.9−303 MPa | | | | | | $-1.17_{\pm0.02}$ | $9_{\pm3}$ | $556_{\pm173}$ |
| | 283 K | 1−402 MPa | | | | | | $-8.2_{\pm0.1}$ | $13_{\pm2}$ | $1247_{\pm115}$ |
| | 283 K | 1−402 MPa | | | | | | $-2.47_{\pm0.01}$ | $29_{\pm6}$ | $2315_{\pm412}$ |

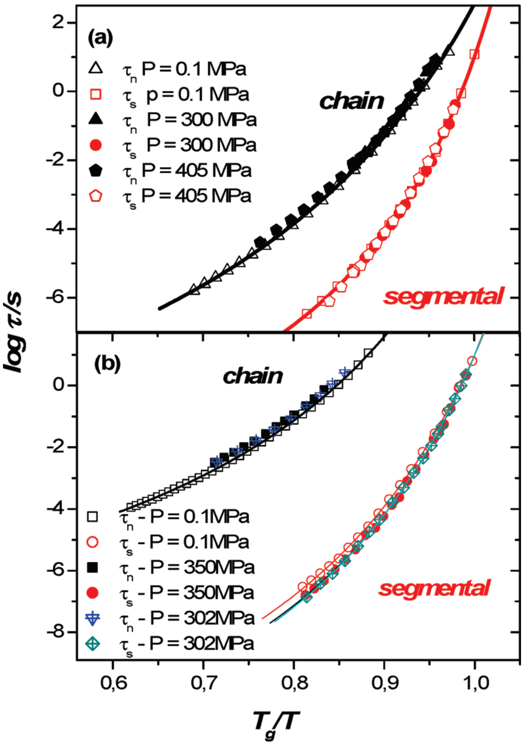

**Figure 5.** Angell plot for relaxation times of both processes for (a) MW = 2.4K and (b) MW = 25K for different isobars.

recently derived from the Avramow model[35]

$$T_g = a\left(1 + \frac{b}{c}P\right)^{1/b} \qquad (2)$$

The obtained parameters are $a = 202.2 \pm 0.8$, $b = 3.1 \pm 0.4$, and $c = 1018.5 \pm 69.3$ for MW = 2.4K and $a = 206.2 \pm 0.2$, $b = 3.05 \pm 0.06$, and $c = 976.7 \pm 10.8$ for MW = 25K. In the limit of zero pressure, the slope is equal to 0.2 ± 0.02 K/MPa for both samples.

Next, our results for different $P-T$ conditions and the different MW were analyzed to determine the relative effects that thermal energy and volume have on both, normal and segmental relaxation times. By combining the dielectric relaxation times for both MW with *PVT* data, we obtain the volume dependencies of the relaxation times for both processes. Figure 7 shows these dependencies for the MW = 25K. The volume behavior of segmental and chain processes strongly depend on thermodynamic path. However, the influence of volume and thermal energy on relaxation dynamics can be quantified by generalized scaling of relaxation times obtained at different thermodynamic conditions, proposed by Casalini et al.[36] The underlying idea of this scaling is that the liquid structure is primarily determined by repulsive forces, with the attractive forces serving as a mean background potential that holds the molecules together. With this form, in principle all thermodynamic properties of the material can be expressed as a function of the $T^{-1}\ V^{-\gamma}$. The magnitude of the material parameter $\gamma$ is correlated with the relative contribution of temperature and volume to the local dynamics. For two extreme cases, volume and thermally activated dynamics, $\gamma = \infty$ and 0, respectively. In polymers temperature is generally the dominating variable for the segmental relaxation, although effect of volume is still important, especially for polymers with more flexible backbone like siloxanes.[5] On the basis of the dielectric isothermal data and the equation of state published by Floudas et al for the PIP with MW = 10.6K,[4] Roland et al. showed that relaxation times for both processes can be scaled on two different curves, but with the same exponent $\gamma = 3.0 \pm 0.15$.[24] They concluded that this small value of $\gamma$ reflects the softness of the intermolecular potential in the investigated polymer.

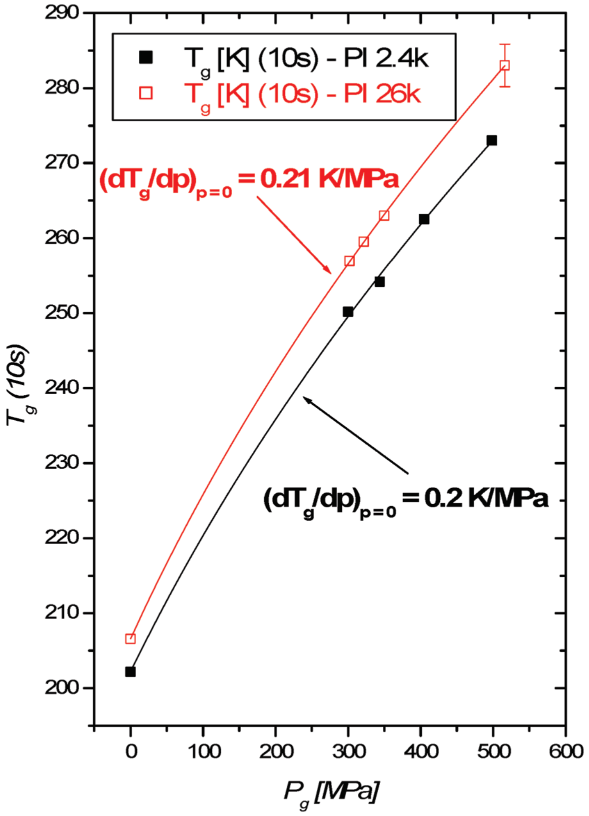

**Figure 6.** Pressure dependence of glass transition temperatures for samples with MW = 2.4K (filled squares) and MW = 25K (empty squares). Solid lines show fits of the data by equation derived from the Avramov model.

We apply the same scaling procedure to volume dependencies of relaxation times for both samples studied here. We emphasize that our measurements cover much broader pressure, temperature and frequency range than data in ref.[4] In the case of the low-MW sample (Figure 8a) data for isobaric and isothermal paths indeed scale on two master curves with the same exponent, although scaling of the segmental relaxation is rather poor, especially at short times limit. Estimated value of $\gamma = 3.5 \pm 0.05$ differs slightly from the value reported by Roland et al. Similar picture emerges for the high-MW sample (Figure 8b): Scaling procedure fails even stronger in the case of segmental relaxation while it works fairly well for the chain relaxation ($\gamma = 3.7 \pm 0.05$). Observed breakdown of the thermodynamic scaling can be related to the difference in the friction mechanisms of segmental and chain modes.

The difference in pressure dependence of chain and segmental modes in PIP have been already reported earlier by Floudas et al.[21] Comparing spectra measured at isothermal conditions, they demonstrated a decrease in the separation between segmental and chain peaks with increase in pressure. This effect is similar to the decrease in separation with decreasing temperature approaching $T_g$. The important new observation in our studies is *the actual increase in separation between segmental and chain relaxation times under pressure at isochronic conditions* (the same segmental relaxation time, Figure 1). Similar effect can be seen also in the earlier data for poly(oxybutylene) (POB) presented in.[22] The separation between both processes can be studied more thoroughly by presenting the ratio $\tau_C/\tau_S$ (i.e., the separation between characteristic times of two modes) as a function of $\tau_S$. This plot (Figure 9) clearly demonstrates a marked increase of the

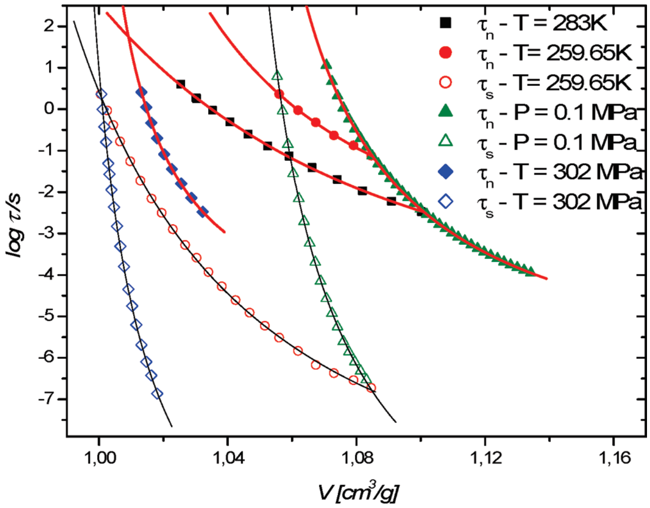

**Figure 7.** Exemplary volume dependences of relaxation times for both segmental and chain processes measured at isothermal and isobaric conditions in the sample with MW = 25K.

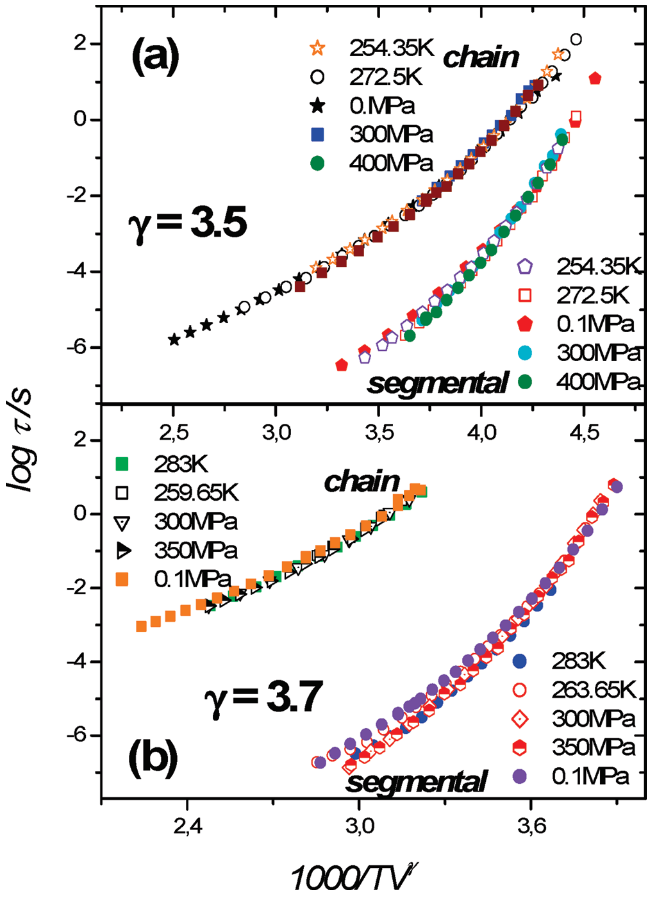

**Figure 8.** Thermodynamic scaling of the relaxation times for segmental and chain modes for the samples with (a) MW = 2.5K and (b) MW = 25K, measured for different $T$ and $P$ conditions.

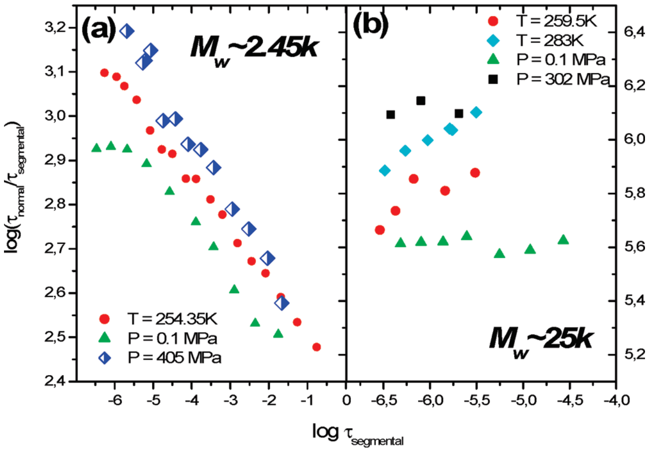

**Figure 9.** Ratio $\tau_C/\tau_S$ vs $\tau_S$ for (a) MW = 2.5k and (b) MW = 25K.

ratio $\tau_C/\tau_S$ with pressure at any given $\tau_S$. The effect seems to decrease upon approaching the glass transition (increase in $\tau_S$) regardless of the thermodynamic paths, isochoric or isothermal.

The ratio $\tau_C/\tau_S$ is much higher for the sample with MW = 25K than for low-MW sample because of larger separation between both relaxations (Figure 9b). For this reason the range of the data accessible for analysis of both processes is strongly limited. Nevertheless, the data clearly demonstrate an increase in the ratio $\tau_C/\tau_S$ at isochronic conditions (Figure 9b). The observed breakdown of time–temperature and time-pressure superposition indicates that the slowing down of segmental relaxation is always stronger than that of the chain relaxation in the region close to the glass transition. However, for the same segmental relaxation times at different P-T conditions, increase in pressure (density) leads to increase in the separation between $\tau_C$ and $\tau_S$. The effect is stronger in higher MW sample: the highest increase in separation is ~2 times for the low-MW sample, while it reaches ~4 times in the high-MW sample.

Here we present a possible explanation of this phenomenon. The dielectrically measured $\tau_C$ corresponds to the relaxation of the end-to-end vector $R_{EE}$ and in nonentangled regime is described by the longest Rouse relaxation time $\tau_R$:[37]

$$\tau_R = \frac{1}{3\pi^2} N^2 a^2 \frac{\xi}{T} \tag{3}$$

Here $N$ is the number and $a$ is the length of the Rouse segments (not the monomers!), $\xi$ is the monomeric friction coefficient. It is usually assumed that segmental dynamics defines the monomeric friction coefficient $\tau_S \propto \xi/T$. Thus, the observed pressure-induced increase in separation between $\tau_S$ and $\tau_C$ at constant $\tau_S$ is most probably caused by the increase in the product $Na$. The dielectric data do not provide enough information to separate these two parameters. However, assuming that the $\langle R_{EE}^2 \rangle$ does not change much with pressure, we can obtain for the Gaussian chain $\langle R_{EE}^2 \rangle = Na^2 \sim$ const. That means that the increase of $N$ is compensated by a slight decrease in length of the Rouse segments $a$. In that case, the ratio $\tau_C/\tau_S \propto N$ for the nonentangled regime. Thus, increase in separation of chain and segmental modes can be caused by an effective increase in the number of the Rouse segments and decrease of their length (although the real length of the chain obviously remains constant). Isochronic conditions (the same $\tau_S$) at higher pressure means higher temperature. As a result, flexibility of the polymer chain might increase leading to an effective decrease in the length of the Rouse segment $a$ and effective increase in $N$. This idea also explains why the increase in separation between chain and segmental dynamics appears even larger in higher MW sample. In this case the chain dynamics is already dictated by reptation and the chain modes have stronger dependence on $N$: $\tau_C \propto N^3$. Thus, we expect even stronger increase in the ratio $\tau_C/\tau_S$. We want to emphasize that the presented above explanation is a speculation, does not have solid justification and other mechanisms of the pressure-induced increase in separation between chain and segmental dynamics measured at isochronic conditions are possible.

As we discussed earlier, the spectra of the segmental relaxation seem to be invariant with pressure (Figure 1). However, the

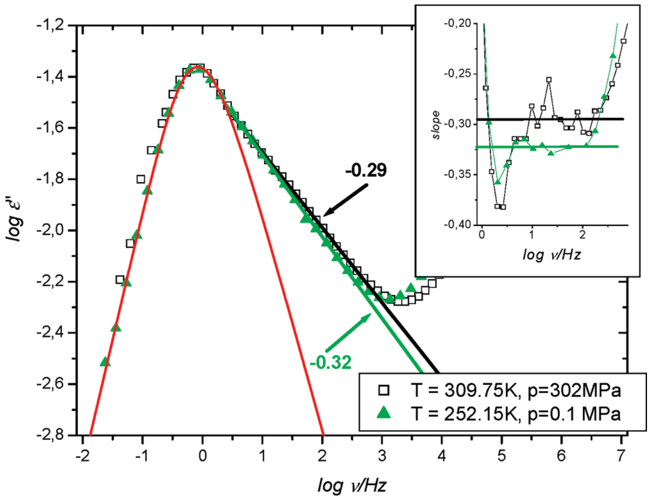

**Figure 10.** Comparison of the chain process' spectral shape in PIP with MW = 25K. Here the data from Figure 8c are superimposed on one curve. Lines depicted fits to the high frequency wings of this process at different thermodynamic conditions. Inset presents derivative analysis of the peak shape.

high-frequency slope of the chain mode clearly decreases with pressure (Figure 1c). This difference is presented better in Figure 10. According to the classical reptation theory, dielectric loss spectrum $\varepsilon''(\nu) \propto G''(\nu)$ and should have high-frequency tail of the normal (chain relaxation) mode $\varepsilon''(\nu) \sim \nu^{-0.5}$, independent of molecular weight.[2,38] However, experimental results accumulated in[27] for PIP demonstrated a molecular weight dependence of the exponent: It varies from $\sim -0.7$ at $M_n \sim 1200$ down to $\sim -0.2$ at $M_n \sim 100\,000$. This unexpected molecular weight dependence of the spectral shape of $\varepsilon''(\nu)$ has not been explained and was emphasized in the recent textbook on dielectric spectroscopy.[39] Our results demonstrate similar tendency with increase in pressure in high-MW sample: the high-frequency slope changes from $-0.32$ at ambient pressure down to $-0.29$ at 302 MPa (Figure 10). This difference is even more obvious in the analysis of the apparent slope of the spectra (inset in Figure 10):

$$\alpha = \frac{\partial \log \varepsilon''(\nu)}{\partial \log \nu}$$

This result is also consistent with the idea of an "effective" increase in the number of Rouse segments.

## Conclusions

Presented here detailed studies of dielectric relaxation in PIP under pressure confirm earlier results on break down of time–temperature and time-pressure superposition. Regardless of the cause (pressure or temperature), segmental dynamics always slows down stronger than chain dynamics on approaching $T_g$. Our analysis did not reveal any significant variations in fragility and spectral shape of the segmental relaxation under pressure. Thermodynamic scaling of the relaxation times ($\log \tau$ vs $T^{-1} V^{-\gamma}$) works fairly well for chain modes, but fails for segmental relaxation, especially for the high-MW sample.

Detailed analysis reveals an increase in separation between chain and segmental dynamics (the ratio $\tau_C/\tau_S$) with pressure at isochronic conditions (the same $\tau_S$). Moreover, clear decrease in the high-frequency slope of the chain spectrum under pressure is observed for the sample with MW = 25K. Both these observations can be explained by an "effective" increase in the number of the Rouse segments $N$ of the chain under pressure at isochronic conditions. It might be caused by a decrease of the Rouse segment length due to higher flexibility of the chain at higher temperature (at isochronic conditions higher pressure is compensated by higher temperature).

**Acknowledgment.** A.S. acknowledges financial support from the NSF Polymer program (DMR-0804571). S.P. acknowledges financial assistance from FNP HOMING program (2008) supported by the European Economic Area Financial Mechanism. M.P. and M.M. acknowledge the support of the Polish Ministry of Sciences and Information Technology Grant No. N202 14732/4240

## References and Notes

(1) Ferry, J. D.; *Viscoelastic Properties of Polymers*, 3rd ed.; John Wiley: New York, 1980.
(2) Doi, M.; Edwards, S. F. *The Theory of Polymer Dynamics*; Clarendon: Oxford, U.K., 1986.
(3) Ngai, K. L.; Plazek, D. J. *Rubber Chem. Technol.* **1995**, *68*, 376.
(4) Floudas, G.; Reisinger, T. *J. Chem. Phys.* **1999**, *111*, 5201.
(5) Paluch, M.; Casalini, R.; Patkowski, A.; Pakula, T.; Roland, C. M. *Phys. Rev. E* **2003**, *68*, 031802.
(6) Roland, C. M.; Casalini, R. *Macromolecules* **2005**, *38*, 8729.
(7) Mierzwa, M.; Floudas, G.; Neidhöfer, G, R.; Spiess, H. W.; Meyer, W. H.; Wegner *J. Chem. Phys.* **2002**, *117*, 6289.
(8) Frick, B.; Dosseh, G.; Cailliaux, A.; Alba-Simionesco, C. *Chem. Phys.* **2003**, *292*, 311.
(9) Kirpatch, A.; Adolf, D. B. *Macromolecules* **2004**, *37*, 1576.
(10) Frick, B.; Alba-Simionesco, C.; Andersen, K. H.; Willner, L. *Phys. Rev. E* **2003**, *67*, 051801.
(11) Tsolou, G.; Harmandaris, V. A.; Mavrantzas, V. G. *J. Chem. Phys.* **2006**, *124*, 084906.
(12) Tsolou, G.; Harmandaris, V. A.; Mavrantzas, V. G. *Macromol. Theory Simul.* **2006**, *15*, 38.
(13) Paluch, M.; Roland, C. M.; Pawlus, S. *J. Chem. Phys.* **2002**, *116*, 10932.
(14) Paluch, M.; Pawlus, S.; Roland, C. M. *Macromolecules* **2002**, *35*, 7338.
(15) Pawlus, S.; Rzoska, S. J.; Ziolo, J.; Paluch, M.; Roland, C. M. *Rubber Chem. Technol.* **2003**, *76*, 1106.
(16) Roland, C. M.; Casalini, R. *Macromolecules* **2003**, *36*, 1361.
(17) Roland, C. M.; Casalini, R.; Santangelo, P.; Sekula, M.; Ziolo, J.; Paluch, M. *Macromolecules* **2003**, *36*, 4954.
(18) Mpoukouvalas, K.; Floudas, G.; Zhang, S. H.; Runt, J. *Macromolecules* **2005**, *38*, 552.
(19) Kriegsa, H.; Gapinski, J.; Meier, G.; Paluch, M.; Pawlus, S.; Patkowski., A. *J. Chem. Phys.* **2006**, *124*, 104901.
(20) Andersson, S. P.; Andersson, O. *Macromolecules* **1998**, *31*, 2999.
(21) Floudas, G.; Gravalides, C.; Reisinger, T. G.; Wegner *J. Chem. Phys.* **1999**, *111*, 9847.
(22) Casalini, R.; Roland, C. M. *Macromolecules* **2005**, *38*, 1779.
(23) Roland, C. M.; Psurek, T.; Pawlus, S.; Paluch, M. *J. Polym. Sci., Part B: Polym. Phys.* **2003**, *41*, 3047.
(24) Roland, C. M.; Paluch, M.; Casalini, R. *J. Polym. Sci. B: Polym. Phys.* **2004**, *42*, 4313.
(25) Ngai, K. L.; Casalini, R.; Roland, C. M. *Macromolecules* **2005**, *38*, 4363.
(26) Adachi, K.; Kotaka, T. *Prog. Polym. Sci.* **1993**, *18*, 585.
(27) Schönhals, A. *Macromolecules* **1993**, *26*, 1309.
(28) Roland, C. M.; Hensel-Bielowka, S.; Paluch, M.; Casalini, R. *Rep. Prog. Phys.* **2005**, *68*, 1405.
(29) Paluch, M.; Rzoska, S. J.; Habdas, P.; Ziolo, J. *J. Phys.:Condens. Matter* **1996**, *8*, 10885.
(30) Paluch, M.; Ziolo, J.; Rzoska, S. J.; Habdas, P. *J. Phys.:Condens. Matter* **1997**, *9*, 5485.
(31) Angell, C. A. In *Relaxations in Complex Systems*; Ngai, K., Wright, G. B., Eds.; National Technical Information Service, U.S. Department of Commerce: Springfield, VA, 1985; p 1.
(32) Ding, Y.; Sokolov, A. P. *Macromolecules* **2006**, *39*, 3322.
(33) Ngai, K. L.; Plazek, D. J.; Roland, C. M. *Macromolecules* **2008**, *41*, 3925.
(34) Sokolov, A. P.; Schweizer, K. S. *Phys. Rev. Lett.* **2009**, *102*, 248301.
(35) Paluch, M.; Hensel-Bielowka, S.; Psurek, T. *J. Chem. Phys.* **2000**, *113*, 4374.
(36) Casalini, R.; Roland, C. M. *Colloid Polym. Sci.* **2004**, *283*, 107.
(37) Strobl, G. *The Physics of Polymers*, 2nd ed.; Springer-Verlag: Berlin and Heidelberg, Germany, 1997.
(38) Watanabe, H. *Macromol. Rapid Commun.* **2001**, *22*, 127.
(39) Kremer, F.; Schönhals, A. *Broadband Dielectric Spectroscopy*; Springer: New York, 2003.